Article

Discovery Medicine 2026; 38(206): 753–766
https://doi.org/10.24976/Discov.Med.202638206.62

Investigating the Protective Effects of Hesperidin on Isoproterenol-Induced Injury in H9c2 Cardiomyocytes via the Akt/GSK3β Pathway

Xiaochun Dai[1], Renhao Chen[2], Ruyi Zhang[1], Wenhe Cai[3], Bobo Li[2], Jiahui Chen[1,*]

[1]Department of Internal Medicine, The Affiliated Kangning Hospital of Wenzhou Medical University, Zhejiang Provincial Clinical Research Center for Mental Disorder, 325000 Wenzhou, Zhejiang, China
[2]Department of Internal Medicine, Wenzhou Yining Elderly Hospital, 325000 Wenzhou, Zhejiang, China
[3]Department of Internal Medicine, Wenzhou Cining Hospital, 325000 Wenzhou, Zhejiang, China
*Correspondence: 13355771872@163.com (Jiahui Chen)
Submitted: 24 October 2025 Revised: 5 January 2026 Accepted: 9 January 2026 Published: 20 March 2026

Background: Isoproterenol (ISO) induces oxidative and apoptotic damage in cardiomyocytes. This study aimed to investigate whether hesperidin (HES) confers a protective effect against ISO-induced injury in H9c2 cardiomyocytes and to determine whether this effect modulates the Protein Kinase B (Akt)/Glycogen Synthase Kinase-3 Beta (GSK3β) signaling pathway.

Methods: H9c2 rat embryonic cardiomyocytes were treated with ISO to establish the optimal injury concentration and with varying HES doses (5, 10, 20 µM) to define a safe and effective range (3-(4,5-dimethylthiazol-2-yl)-2,5-diphenyltetrazolium bromide, MTT assay). The cells were divided into five groups: Control, ISO alone, and ISO plus HES at each concentration. The viability and proliferative capacity of the cells were assessed using MTT and 5-Ethynyl-2′-deoxyuridine (EdU) assays. Markers of injury and oxidative stress—Lactate dehydrogenase (LDH) release, glutathione (GSH), catalase (CAT), and malondialdehyde (MDA) levels, superoxide dismutase (SOD) activity, and intracellular reactive oxygen species (ROS)—were measured. Apoptosis and mitochondrial function were assessed using Terminal deoxynucleotidyl transferase dUTP nick end labeling (TUNEL) staining, 5,5′,6,6′-tetrachloro-1,1′,3,3′-tetraethylbenzimidazolylcarbocyanine iodide (JC-1) dye for membrane potential, and Western blotting for B-cell lymphoma 2 (Bcl-2), Bcl-2-associated X protein (Bax), Cysteine-aspartic acid protease-3 (caspase-3), PTEN-induced putative kinase 1 (PINK1), Parkin and cytochrome C. Akt/GSK3β pathway activation was analyzed using quantitative real-time polymerase chain reaction (qRT-PCR) and phospho-specific Western blotting. The role of Akt was confirmed by co-treatment with the Akt-specific inhibitor VIII.

Results: Compared to ISO alone, HES dose-dependently enhanced cell viability and proliferation, significantly reduced LDH release, MDA, and ROS levels, while increasing GSH and CAT levels, as well as SOD activity ($p < 0.05$). Results from the TUNEL assay and JC-1 staining demonstrated that treatment with HES markedly reduced the proportion of apoptotic cells and effectively maintained the integrity of the mitochondrial membrane potential ($p < 0.05$). Western blot analysis showed that HES treatment upregulated the levels of anti-apoptotic protein Bcl-2 and mitochondrial quality control proteins PINK1 and Parkin, while downregulating the levels of pro-apoptotic proteins Bax, caspase-3, and cytochrome C ($p < 0.05$). Treatment with HES notably enhanced the phosphorylation levels of both Akt and GSK3β proteins ($p < 0.05$), indicating activation of this signaling cascade. These protective effects were abolished in the presence of Akt inhibitor VIII, confirming reliance on Akt/GSK3β signaling.

Conclusion: Hesperidin exerts significant cardioprotective effects by alleviating ISO-induced oxidative stress, mitochondrial impairment, and apoptotic injury in H9c2 cardiomyocytes, an effect largely attributed to its activation of the Akt/GSK3β signaling pathway, thereby highlighting its therapeutic potential in cardiac protection.

Keywords: hesperidin; isoproterenol; myocardial injury; oxidative stress; apoptosis; Akt/GSK3β pathway

Introduction

Cardiovascular diseases remain a leading cause of mortality and morbidity in China, with high rates of disability and death imposing a significant health burden [1]. Despite the adoption of advanced therapeutic strategies, myocardial injury often occurs as an unavoidable outcome. Among various pathological mechanisms, mitochondrial dysfunction has been identified as a major contributor to ischemic myocardial injury [2]. Abnormalities in mitochondrial energy metabolism, structure, and dynamics are closely associated with cardiac dysfunction [3,4]. Disruption of mitochondrial homeostasis contributes to myocardial hypertrophy, arrhythmia, and heart failure, yet the underlying molecular mechanisms remain largely unclear [5].

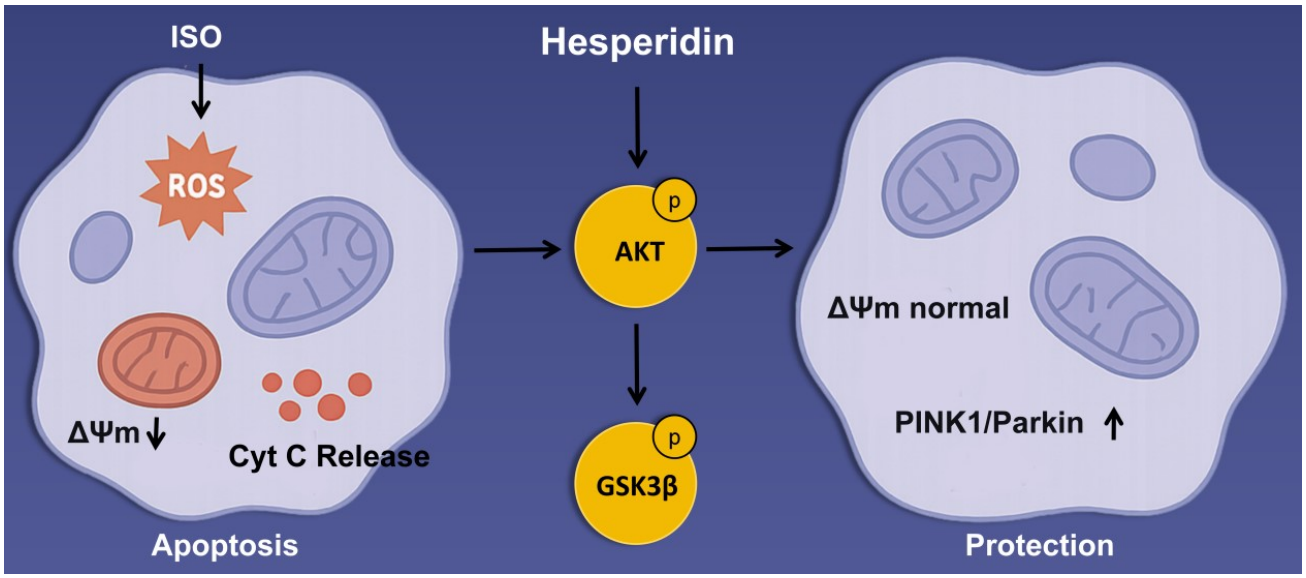

Graphical Abstract.

Therefore, clarifying the regulatory network of mitochondrial metabolism and identifying novel therapeutic targets are critical for preventing myocardial injury.

Although several anti-ischemic drugs are available in clinical practice, their efficacy and safety profiles are limited, and novel agents with multitarget regulatory actions are urgently needed [6]. Traditional Chinese medicine (TCM) offers unique advantages due to its holistic and multitarget pharmacological properties [7]. Growing evidence indicates that TCM can modulate myocardial energy metabolism, suppress oxidative stress and apoptosis, alleviate inflammation, and improve endothelial function during myocardial ischemia [8]. These multifaceted effects suggest that TCM-derived compounds may offer therapeutic potential for mitochondrial protection and cardiomyocyte survival.

Hesperidin (HES), a flavonoid glycoside abundantly present in citrus fruits, has garnered increasing attention for its cardiovascular protective effects. As a bioactive polyphenolic compound, HES exhibits antioxidative, anti-inflammatory, antihypertensive, and hypolipidemic activities [9,10]. Accumulating evidence supports its potential to improve multiple cardiovascular risk factors, making it a promising candidate for myocardial protection [11]. However, studies specifically examining the protective effects and molecular mechanisms of HES in isoproterenol (ISO)-induced myocardial injury remain limited.

Recent findings suggest that the PI3K/Protein Kinase B (Akt)/Glycogen Synthase Kinase-3 Beta (GSK3β) signaling pathway plays a pivotal role in regulating mitochondrial function and cardiomyocyte apoptosis [12–14]. Activation of Akt leads to phosphorylation of GSK3β at Ser9, resulting in its inactivation and subsequent inhibition of apoptosis, thereby exerting cardioprotective effects [15–18]. Based on these findings, we hypothesize that HES may mitigate ISO-induced myocardial injury by activating the Akt/GSK3β signaling pathway and restoring mitochondrial homeostasis. This study aims to elucidate the molecular mechanisms underlying the cardioprotective effects of HES in H9c2 cells, providing experimental evidence for its potential application in ischemic heart disease.

Materials and Methods

Cell Culture

Rat embryonic myocardial cells (H9c2, CL-0089) were sourced from Wuhan Procell Life Science & Technology Co., Ltd (Wuhan, China). Short tandem repeat profiling was performed to authenticate the cell line, and mycoplasma contamination testing confirmed that the cells were free of infection. The H9c2 cells were grown in Dulbecco's Modified Eagle Medium (DMEM, high glucose, 11965092, Thermo Fisher, Waltham, MA, USA), supplemented with 10% fetal bovine serum (FBS, A5669401, Thermo Fisher, Waltham, MA, USA) and 1% penicillin-streptomycin solution (C0222, Beyotime, Shanghai, China). Cell cultures were incubated under standard conditions at 37 °C in a 5% CO_2 atmosphere with saturated humidity. Cells in the exponential growth phase and exhibiting optimal morphology were selected for experimental use.

Cell Treatment and Grouping

H9c2 cells exhibiting uniform growth and appropriate confluency were randomly assigned to five experimental groups. In the Control group (Control): Cells were cultured under standard conditions without any special treatment, serving as the normal control. ISO group: Cells were treated with 10 μM ISO (1351005, purity ≥98.5%, Sigma-Aldrich, St. Louis, MO, USA) in DMEM (11965092,

Thermo Fisher, Waltham, MA, USA) containing 10% FBS (A5669401, Thermo Fisher, Waltham, MA, USA) for 24 hours to simulate the pathological state induced by ISO.

HES groups: Based on the ISO group, cells were further treated with HES (MB5810-1, MeilunBio, Dalian, China) at final doses of 5, 10, and 20 µM, respectively, in DMEM (11965092, Thermo Fisher, Waltham, MA, USA) supplemented with 10% FBS (A5669401, Thermo Fisher, Waltham, MA, USA).

3-(4,5-dimethylthiazol-2-yl)-2,5-diphenyltetrazolium bromide (MTT) Assay

The MTT assay was conducted to determine the optimal ISO concentration for inducing myocardial injury and to evaluate the cytotoxicity and safe concentration range of HES.

(1) Determination of ISO concentration: H9c2 cardiomyocytes were plated in 96-well plates at a density of 5×10^4 cells per well and cultured for 24 hours. Cells were then exposed to various concentrations of ISO (2.5, 5, 10, 20, and 40 µM) [19] for 24 hours. Cell viability was assessed using the MTT assay (M8180, Solarbio, Beijing, China), and absorbance was recorded at 492 nm with a microplate spectrophotometer (CMaxPlus, Molecular Devices, USA). The inhibition rate was calculated, and 10 µM ISO was identified as the optimal concentration for inducing reproducible cell injury with moderate viability reduction.

(2) Determination of the safe concentration of HES: Similarly, cells were treated with different concentrations of HES (5, 10, 20, 40, 60, 80, and 100 µM) [20] for 24 hours to evaluate cytotoxicity. Cell viability was measured via the same MTT method, and concentrations below 20 µM exhibited no significant cytotoxic effects.

(3) Effect of Akt inhibitor VIII: To evaluate the effect of Akt signaling inhibition, H9c2 cells were treated with various concentrations of Akt inhibitor VIII (0.1, 0.2, 0.5, 1, and 2 µM) [21], and cell viability was assessed using the MTT assay as described above.

Based on these results, cells were randomly divided into five groups for subsequent experiments: Control, ISO, and HES (5, 10, and 20 µM). The Control group was cultured in high-glucose DMEM alone; the ISO group was treated with 10 µM ISO for 24 hours; and the HES groups received 5, 10, or 20 µM HES in combination with ISO for 24 hours.

5-Ethynyl-2′-deoxyuridine (EdU) Cell Proliferation Assay

Cells were cultured with 10 µM EdU at 37 °C for 2 h, fixed with 4% paraformaldehyde (P1110, Solarbio, Beijing, China) for 10 min, washed with phosphate-buffered saline (PBS) (P1020, Solarbio, Beijing, China), and permeabilized with 0.5% Triton X-100 (0694, LABLEAD, Beijing, China) for 10 min. The click reaction was performed according to the EdU Kit protocol (C0075S, Beyotime, Shanghai, China). Nuclei were stained with 1 µg/mL 4′,6-diamidino-2-phenylindole (DAPI, C1002, Beyotime, Shanghai, China) for 10 min at room temperature (RT) in the dark. Fluorescence images were acquired using a fluorescence microscope (CKX53, OLYMPUS, Tokyo, Japan). EdU-positive cell percentage was quantified by ImageJ (version 1.46; National Institutes of Health, Bethesda, MD, USA) to assess proliferation.

Biochemical Assays

The culture media supernatants from each H9c2 cell group were harvested, and the levels of Lactate dehydrogenase (LDH) (C0016, Beyotime, Shanghai, China) release, superoxide dismutase (SOD) (BC5165, Solarbio, Beijing, China) activity, malondialdehyde (MDA) (BC0025, Solarbio, Beijing, China) content, glutathione (GSH) (S0053, Beyotime, Shanghai, China) levels, and catalase (CAT) (BC0205, Solarbio, Beijing, China) activity were determined following the manufacturers' protocols.

2′,7′-Dichlorodihydrofluorescein Diacetate (DCFH-DA) Assay

Following treatment, culture medium was removed from each H9c2 group, and cells were washed thrice with PBS. Then, 1 mL of 10 µM DCFH-DA (CA1410, Solarbio, Beijing, China) was added per well. After 30-min incubation at 37 °C, the dye was removed, and cells were washed twice with PBS. For nuclear counterstaining, cells were incubated with DAPI solution (C1002, Beyotime, Shanghai, China) for 5 min at room temperature and rinsed gently with PBS. Fluorescence images were captured with a fluorescence microscope (CKX53, OLYMPUS, Tokyo, Japan), and intensity was quantified via ImageJ (V1.46; National Institutes of Health, USA).

TUNEL Assay

Cells were fixed in 4% paraformaldehyde for 10 min, rinsed with PBS, and then permeabilized using 0.3% Triton X-100 for 5 min at RT. Cells were then incubated with TUNEL solution (T2195, Solarbio, Beijing, China) for 1 h at 37 °C in the dark. Nuclei were stained with 1 µg/mL DAPI for 10 min at RT, protected from light. Fluorescence images were acquired using a fluorescence microscope (CKX53, OLYMPUS, Tokyo, Japan). The proportion of TUNEL-positive cells was quantified with ImageJ (V1.46; National Institutes of Health, USA) to assess apoptosis.

Mitochondrial Membrane Potential (MMP) Detection

A 5,5′,6,6′-Tetrachloro-1,1′,3,3′-tetraethylbenzimidazolylcarbocyanine iodide (JC-1) staining buffer (1×) was prepared by diluting 5× JC-1 buffer (C2006, Beyotime, Shanghai, China) with distilled

water at a ratio of 1:4 and kept on ice. After treatment, cells were washed twice with PBS. Cells were incubated with JC-1 working solution, and incubated at 37 °C for 20 min. The supernatant was discarded, followed by two washes of the cells with 1× JC-1 buffer. Ultimately, 2 mL of culture medium was introduced into each well. Fluorescence images were immediately captured using an inverted fluorescence microscope (CKX53, OLYMPUS, Tokyo, Japan).

Quantitative Real-Time Polymerase Chain Reaction (qRT-PCR)

Total RNA was isolated from each group utilizing a total RNA extraction reagent (R0016, Beyotime, Shanghai, China). Subsequently, the extracted RNA was reverse-transcribed into cDNA using a reverse transcription kit (KR116, Tiangen Biotech, Beijing, China). Quantitative PCR was conducted employing specific forward and reverse primers on a real-time PCR instrument (LightCycler96, Roche, Switzerland), with β-actin serving as an internal reference. Gene expression was quantified via the $2^{-\Delta\Delta CT}$ method; primer sequences are shown in Table 1.

Table 1. Primer information.

Gene	Primer sequence (5′→3′)
Akt	F: TACCTGAAGCTACTGGGCAAGGG
	R: CGGTCGTGGGTCTGGAATGAG
GSK3β	F: CCAGGTGGAGGACCATTTGC
	R: ACTCTACACCAGCAGCAGCC
β-actin	F: TCAGGTCATCACTATCGGCAAT
	R: AAAGAAAGGGTGTAAAACGCA

Akt, *Protein Kinase B*; *GSK3β*, *Glycogen Synthase Kinase-3 Beta*.

Western Blotting (WB)

After treatment, H9c2 cells underwent triple PBS rinses and were subsequently lysed on ice for 30 min using radioimmunoprecipitation assay (RIPA) buffe (P0013C, Beyotime, Shanghai, China) to obtain total protein extracts. Proteins were then separated using sodium dodecyl sulfate-polyacrylamide gel electrophoresis (SDS-PAGE) (P0015A, Beyotime, Shanghai, China) and subsequently transferred to polyvinylidene fluoride (PVDF) membranes. After blocking, membranes were treated with the following primary antibodies diluted 1:1000 as follows: B-cell lymphoma 2 (Bcl-2, GB153375, Servicebio, Wuhan, China), Bcl-2-associated X protein (Bax, GB12690, Servicebio, Wuhan, China), Cleaved cysteine-aspartic protease 3 (p-Caspase-3, PA5-118735, Thermo Fisher, Waltham, MA, USA), Caspase-3 (19677-1-AP, Proteintech, Wuhan, China), Cytochrome c (Cyto-C, GB12080, Servicebio, Wuhan, China), p-Akt (66444-1-Ig, Proteintech, Wuhan, China), Akt (10176-2-AP, Proteintech, Wuhan, China), p-GSK3β (GB114582, Servicebio, Wuhan, China), GSK3β (82061-1-RR, Proteintech, Wuhan, China), and β-actin (66009-1-Ig, Proteintech, Wuhan, China). After incubation with HRP-conjugated secondary antibody (SA00001-1-A, SA00001-4, Proteintech, Wuhan, China), protein bands were detected via enhanced chemiluminescence (P0018S, Beyotime, Shanghai, China) using the Fusion FX7 imaging platform (Peqlab, Erlangen, Germany). The relative intensity of each band was analyzed and measured with ImageJ software (V1.46; National Institutes of Health, USA).

Akt/GSK3β Pathway Inhibition Assay

To verify whether HES activates the Akt/GSK3β signaling pathway, the Akt-specific inhibitor VIII (abs810176, Absin, Shanghai, China) was employed in subsequent experiments. Based on a preliminary gradient inhibition assay (0.1, 0.2, 0.5, 1, and 2 µM), 0.1 µM was identified as the optimal concentration [21], effectively suppressing Akt phosphorylation without inducing cytotoxicity. After ISO treatment, H9c2 cells were pretreated with 0.1 µM Akt inhibitor VIII for 30 min, followed by co-treatment with HES at its maximum concentration (20 µM) for an additional 24 hours. Cells were then collected for further analysis.

Statistical Analysis

All experiments were independently repeated at least three times. For each biological replicate, measurements were performed in triplicate technical replicates. Statistical analysis was performed using GraphPad Prism version 9.5 (GraphPad Software, La Jolla, CA, USA). Data are expressed as the mean ± standard deviation ($\bar{x} = \pm$ SD). Prior to analysis, data were tested for normality using the Shapiro-Wilk test and for homogeneity of variance using Levene's test. One-way ANOVA was performed for comparisons among multiple groups when assumptions of normality and homogeneity of variance were met. If these assumptions were not satisfied, appropriate non-parametric tests (such as the Kruskal-Wallis test) were used instead. A $p < 0.05$ was considered a statistically significant difference.

Results

HES Attenuates ISO-Induced Injury in H9c2 Cardiomyocytes

As demonstrated by the MTT assay, cell viability declined progressively in a concentration-dependent manner following 24 hours of exposure to ISO at concentrations ranging from 2.5 to 40 µM. At 10 µM, cell viability decreased to approximately 60%, indicating substantial myocardial injury, and damage became more pronounced at a concentration ≥20 µM (Fig. 1A, $p < 0.05$). Therefore, ISO at a concentration of 10 µM was selected for establishing the cardiomyocyte injury model. Different levels of

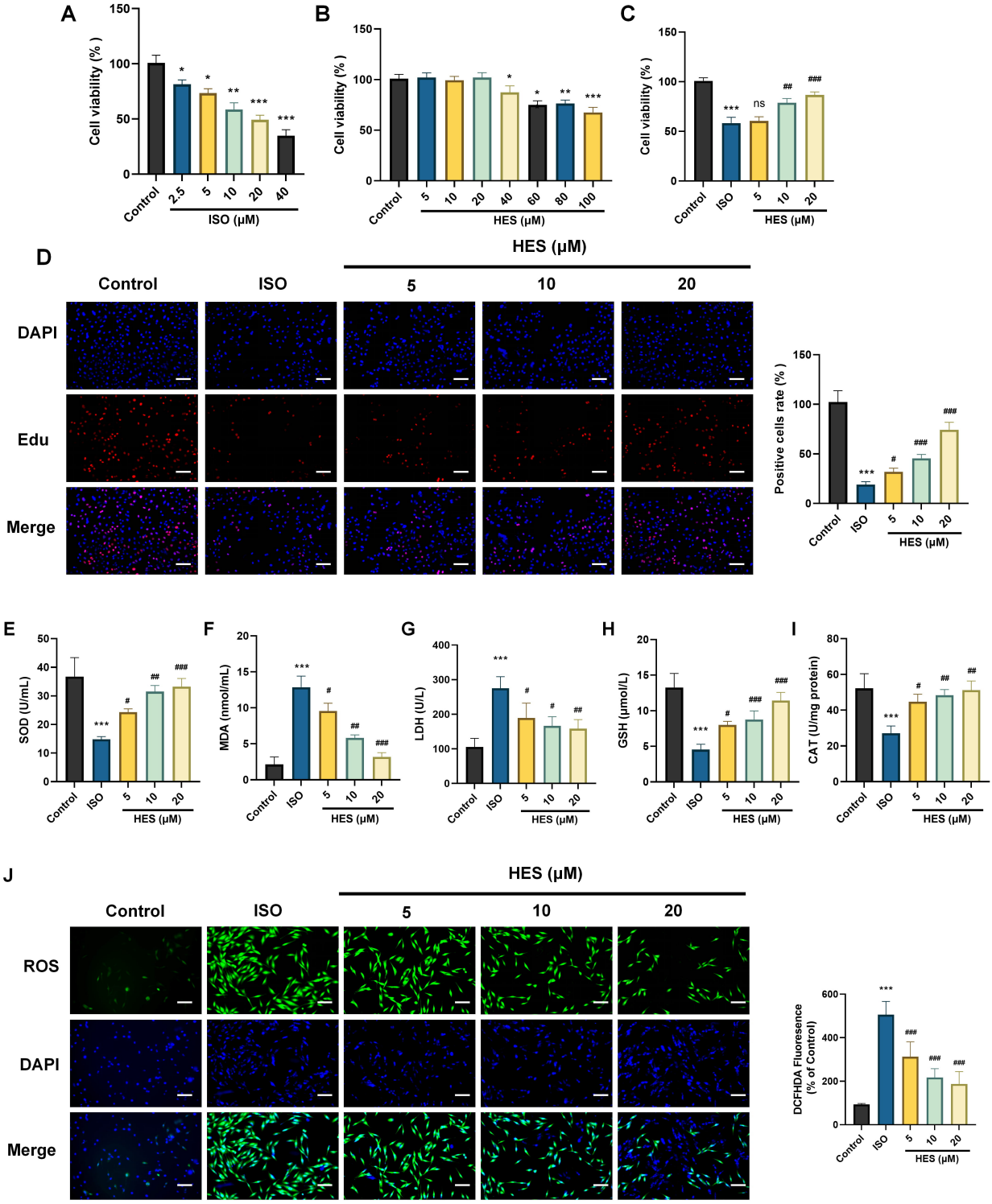

Fig. 1. Impact of HES on ISO-triggered damage in H9c2 cardiomyocytes. (A) Survival rate of H9c2 cells following 24 h treatment with varying concentrations of ISO. (B) Cell viability following treatment with increasing concentrations of HES. (C) HES-mediated protection against ISO-triggered cytotoxicity in H9c2 cells. (D) EdU assay assessing HES's influence on ISO-reduced cell proliferation in H9c2 cells (200× magnification, scale bar: 50 μm). (E) Activity of SOD. (F) Levels of MDA. (G) Release of LDH. (H) GSH levels. (I) CAT levels. (J) Intracellular ROS detected via DCFH-DA staining (400× magnification, scale bar: 25 μm). Data are presented as mean ± SD, n = 3. $^{*}p < 0.05$, $^{**}p < 0.01$, $^{***}p < 0.001$ vs. Control; ns, not significant; $^{\#}p < 0.05$, $^{\#\#}p < 0.01$, $^{\#\#\#}p < 0.001$ vs. ISO. HES, hesperidin; ISO, Isoproterenol; EdU, 5-Ethynyl-2′-deoxyuridine; SOD, superoxide dismutase; MDA, malondialdehyde; LDH, Lactate dehydrogenase; GSH, glutathione; CAT, catalase; DCFH-DA, 2′,7′-Dichlorodihydrofluorescein diacetate.

HES (5–100 μM) alone were applied to H9c2 cells; concentrations ≤20 μM exhibited no significant cytotoxicity, whereas concentrations ≥40 μM notably suppressed cell viability (Fig. 1B, $p < 0.05$). Therefore, HES concentrations of 5, 10, and 20 μM were selected as the working concentrations for the following experimental procedures. Upon co-treatment with ISO and increasing concentrations of HES, cell viability was progressively restored (Fig. 1C, $p < 0.05$).

In the EdU proliferation assay, the nuclei of the Control group exhibited blue staining by DAPI, and proliferating cells exhibited strong red fluorescence due to EdU incorporation. Compared with the Control group, cells in the ISO-treated group showed a significant reduction in the number of red EdU-positive nuclei, reflecting a marked suppression of cellular proliferative activity. In contrast, HES administration increased the number of EdU-positive cells relative to the ISO group, demonstrating a significant enhancement of proliferative capacity (Fig. 1D, $p < 0.05$). These findings demonstrate that HES effectively restores ISO-impaired cell viability and proliferation in H9c2 cardiomyocytes.

To elucidate the protective effects of HES against ISO-induced injury in H9c2 cardiomyocytes, key oxidative stress-related markers were evaluated. Compared with the Control group, ISO treatment significantly suppressed antioxidant defenses (SOD activity, GSH and CAT levels), while markedly increasing MDA levels, LDH release, and intracellular ROS levels, indicating pronounced oxidative stress and membrane damage. All five parameters improved to varying extents after treatment with HES at concentrations of 5, 10, and 20 μM. Notably, the HES groups demonstrated significant restoration of SOD activity, GSH and CAT levels, alongside substantial reductions in MDA, LDH, and ROS levels (Fig. 1E–J, $p < 0.05$). The findings indicate that HES can significantly reduce ISO-triggered oxidative damage and cell injury in H9c2 cardiomyocytes, demonstrating a protective effect that increases with dosage.

HES Ameliorates ISO-Induced Mitochondrial Dysfunction and Apoptosis in H9c2 Cells

TUNEL staining revealed a significant increase in apoptotic nuclei in the ISO group compared with the Control group, while HES treatment markedly reduced the number of TUNEL-positive cells, indicating effective suppression of ISO-induced apoptosis (Fig. 2A, $p < 0.05$). JC-1 staining showed that ISO exposure induced a marked loss of MMP, reflected by a decreased red-to-green fluorescence ratio, whereas HES significantly restored MMP levels, suggesting protection of mitochondrial integrity (Fig. 2B, $p < 0.05$).

Western blot results demonstrated that ISO significantly upregulated pro-apoptotic proteins (Bax, p-Caspase-3/Caspase-3, and Cytochrome C) while downregulating the anti-apoptotic protein Bcl-2 and mitochondrial quality control–associated proteins PINK1 and Parkin ($p < 0.05$). HES treatment effectively reversed these changes, restoring Bcl-2 levels, enhancing PINK1 and Parkin expression, and reducing Bax, p-Caspase-3/Caspase-3, and Cytochrome C levels (Fig. 2C, $p < 0.05$).

Collectively, these findings suggest that HES attenuates ISO-induced mitochondrial apoptosis and improves mitochondrial homeostasis, potentially through activation of the Akt/GSK3β signaling pathway, thereby exerting cardioprotective effects.

HES Mitigates ISO-Induced Damage in H9c2 Cardiomyocytes Through Activation of the Akt/GSK3β Pathway

Western blot analysis showed that ISO treatment significantly decreased the phosphorylation ratios of p-Akt/Akt and p-GSK3β/GSK3β compared with the Control group; HES treatment, particularly at concentrations of 10 μM and 20 μM, restored these phosphorylation levels in a concentration-dependent manner (Fig. 3A,B; $p < 0.05$), indicating reactivation of the Akt/GSK3β pathway.

Consistent with the protein data, qRT-PCR analysis demonstrated that ISO suppressed the mRNA expression of Akt and GSK3β, whereas HES significantly upregulated their transcription (Fig. 3C, $p < 0.05$). These results suggest that the cytoprotective effects of HES against ISO-induced damage are, at least in part, mediated through activation of the Akt/GSK3β signaling cascade.

Suppression of Akt Signaling Diminishes HES's Protective Impact Against ISO-Triggered Injury in H9c2 Cardiomyocytes

To further confirm the involvement of the Akt/GSK3β signaling pathway in HES-mediated cardioprotective effects, Akt inhibitor VIII was used. H9c2 cells were treated with varying concentrations of the inhibitor (0.1, 0.2, 0.5, 1, and 2 μM), and Western blot analysis showed that 0.1 μM was sufficient to markedly suppress Akt phosphorylation without causing significant cytotoxicity (Fig. 4A,B; $p < 0.05$). Higher concentrations did not further inhibit Akt, and slightly reduced cell viability; therefore, 0.1 μM was chosen for subsequent experiments.

Cells were then assigned to four groups: ISO, ISO + HES (20 μM), ISO + Akt inhibitor (0.1 μM), and ISO + HES (20 μM) + Akt inhibitor (0.1 μM). MTT and EdU assays revealed that HES treatment significantly improved cell viability and proliferation compared with ISO alone. However, Akt inhibition partially reversed these protective effects of HES, as indicated by reduced cell viability and fewer EdU-positive cells in the ISO + HES + inhibitor group (Fig. 4C–E; $p < 0.05$).

Consistently, HES markedly enhanced antioxidant enzyme activities, including SOD, GSH, and CAT, and decreased oxidative stress markers (MDA, LDH, ROS) relative to ISO alone. Co-treatment with Akt inhibitor VIII at-

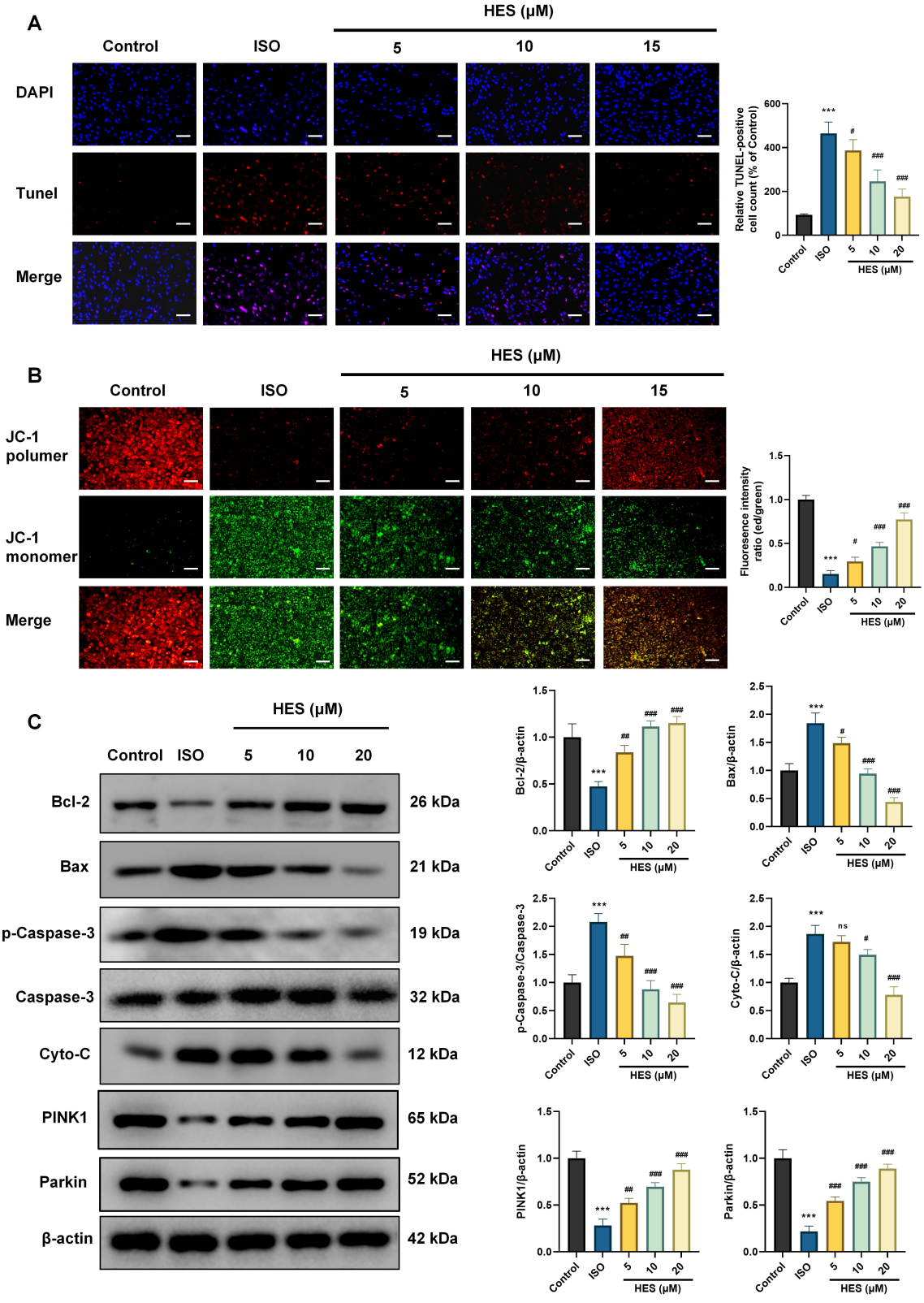

Fig. 2. Effects of HES on mitochondria-mediated apoptosis in ISO-treated H9c2 cardiomyocytes. (A) Apoptosis levels detected by Terminal deoxynucleotidyl transferase dUTP nick end labeling (TUNEL) staining (200× magnification, scale bar: 50 μm). (B) Mitochondrial membrane potential (MMP) assessed via 5,5′,6,6′-tetrachloro-1,1′,3,3′-tetraethylbenzimidazolylcarbocyanine iodide (JC-1) staining (200× magnification, scale bar: 50 μm). (C) Expression of mitochondrial apoptosis–related proteins and mitochondrial homeostasis–associated proteins analyzed by Western Blotting (WB). Data are presented as mean ± SD, n = 3. ***$p < 0.001$ vs. Control; ns, not significant; $^{\#}p < 0.05$, $^{\#\#}p < 0.01$, $^{\#\#\#}p < 0.001$ vs. ISO.

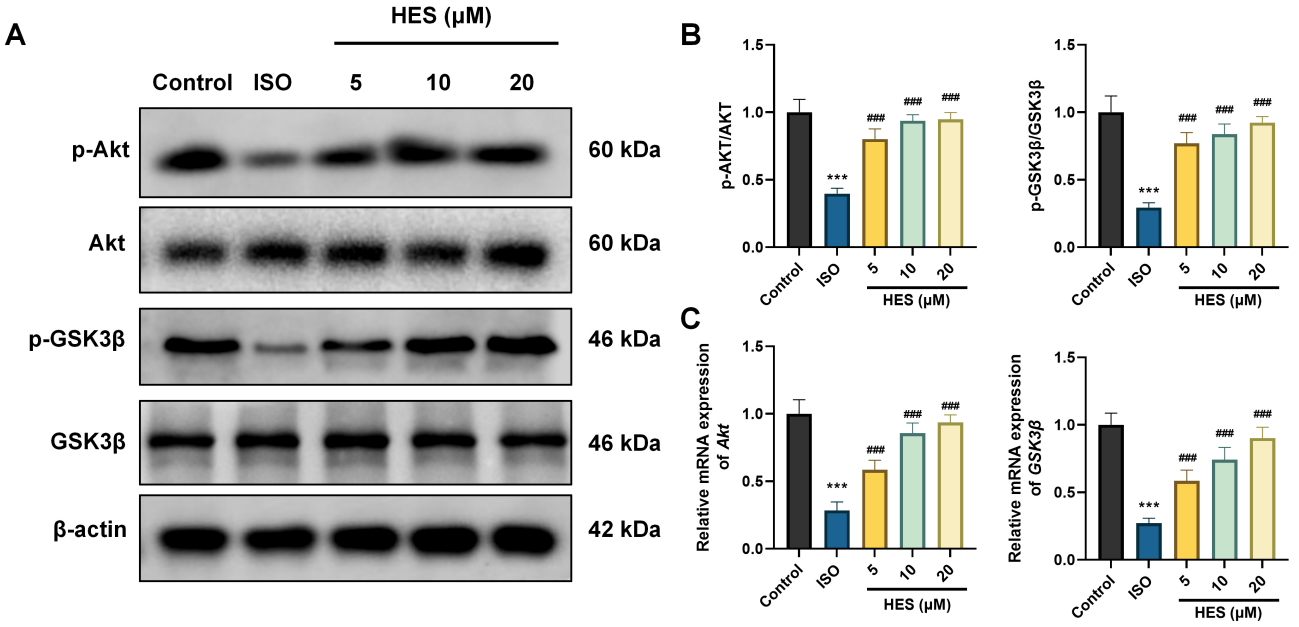

Fig. 3. The regulatory influence of HES on the Akt/GSK3β signaling pathway in H9c2 cardiomyocytes subjected to ISO treatment. (A) WB analysis of Akt/GSK3β pathway-associated protein expression. (B) WB band intensity analysis. (C) Quantitative real-time polymerase chain reaction (qRT-PCR)-based measurement of the mRNA levels of *Akt* and *GSK3β* in H9c2 cardiomyocytes. Data are presented as mean ± SD, n = 3. ***$p < 0.001$ vs. Control; $^{###}p < 0.001$ vs. ISO.

tenuated these antioxidant effects, resulting in lower SOD, GSH, and CAT levels and higher MDA, LDH, and ROS levels compared with the ISO + HES group (Fig. 4F–K; $p < 0.05$).

These results indicate that the protective and antioxidant effects of HES are at least partially mediated through activation of the Akt/GSK3β signaling pathway.

Akt Signaling Pathway Plays a Central Role in HES's Mitigation of Mitochondrial Impairment and Apoptotic Cell Death Induced by ISO

TUNEL staining revealed a significant reduction in apoptotic cells in the ISO + HES group compared with ISO alone (Fig. 5A, $p < 0.05$), indicating a potent anti-apoptotic effect of HES. Co-treatment with Akt inhibitor VIII markedly increased apoptosis, partially reversing the protective effect of HES.

Consistently, JC-1 staining showed that HES significantly restored mitochondrial membrane potential, evidenced by an increased red-to-green fluorescence ratio compared with ISO alone, whereas Akt inhibition attenuated this improvement (Fig. 5B; $p < 0.05$).

Western blot analysis further confirmed these findings. Compared with ISO alone, HES treatment upregulated the anti-apoptotic protein Bcl-2 and mitochondrial quality control proteins PINK1 and Parkin, while reducing pro-apoptotic markers Bax, p-Caspase-3/Caspase-3, and Cytochrome C. These protective effects of HES were partially reversed by Akt inhibitor VIII (Fig. 5C; $p < 0.05$).

Collectively, these results indicate that HES mitigates apoptosis and mitochondrial dysfunction in H9c2 cardiomyocytes, at least in part through activation of the Akt/GSK3β signaling pathway.

Akt Inhibitor VIII Attenuates the HES-Induced Activation of the Akt/GSK3β Pathway

WB analysis revealed that p-Akt/Akt and p-GSK3β/GSK3β levels were markedly elevated in the ISO + HES group compared with ISO alone, indicating that HES effectively activates the Akt/GSK3β signaling pathway. However, co-treatment with Akt inhibitor VIII significantly reduced the phosphorylation of Akt and GSK3β, thereby attenuating the activation of this pathway and partially reversing the effect of HES (Fig. 6A,B, $p < 0.05$). Consistent with the WB results, qRT-PCR analysis showed that HES significantly upregulated the mRNA expression of Akt and GSK3β compared with ISO treatment alone, whereas the co-treatment with Akt inhibitor VIII diminished these increases (Fig. 6C, $p < 0.05$).

Collectively, these findings indicate that HES confers cytoprotective effects in H9c2 cardiomyocytes primarily through activation of the Akt/GSK3β signaling pathway, while pharmacological inhibition of Akt markedly weakens this protective effect.

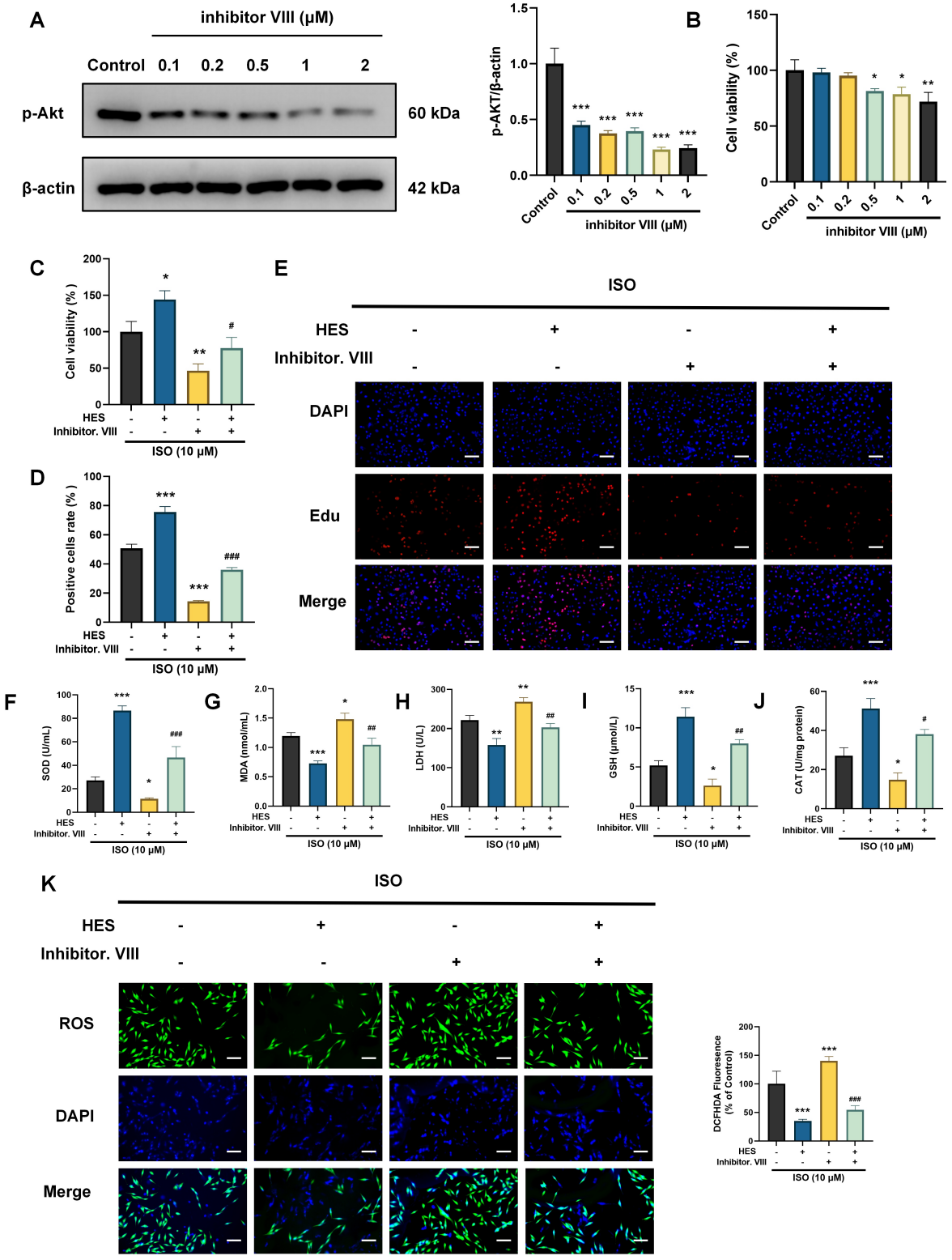

Fig. 4. Inhibition of Akt signaling via inhibitor VIII compromises HES-mediated protection against ISO-triggered damage in H9c2 cells. (A) WB analysis showing inhibition of Akt phosphorylation by Akt inhibitor VIII at concentrations of 0.1, 0.2, 0.5, 1, and 2 μM (n = 3). (B,C) MTT assay evaluating cell viability. (D) Measurement of cell proliferation through the EdU assay (n = 3). (E) Representative images of EdU staining (n = 3, 200× magnification, scale bar: 50 μm). (F) Activity of SOD. (G) MDA concentration. (H) LDH release level. (I) GSH levels. (J) CAT levels. (K) ROS fluorescence intensity in H9c2 cells (400× magnification, scale bar: 25 μm). Data are presented as mean ± SD, n = 3. *$p < 0.05$, **$p < 0.01$, ***$p < 0.001$ vs. ISO group; $^{\#}p < 0.05$, $^{\#\#}p < 0.05$, $^{\#\#\#}p <$ 0.001 vs. ISO + HES group.

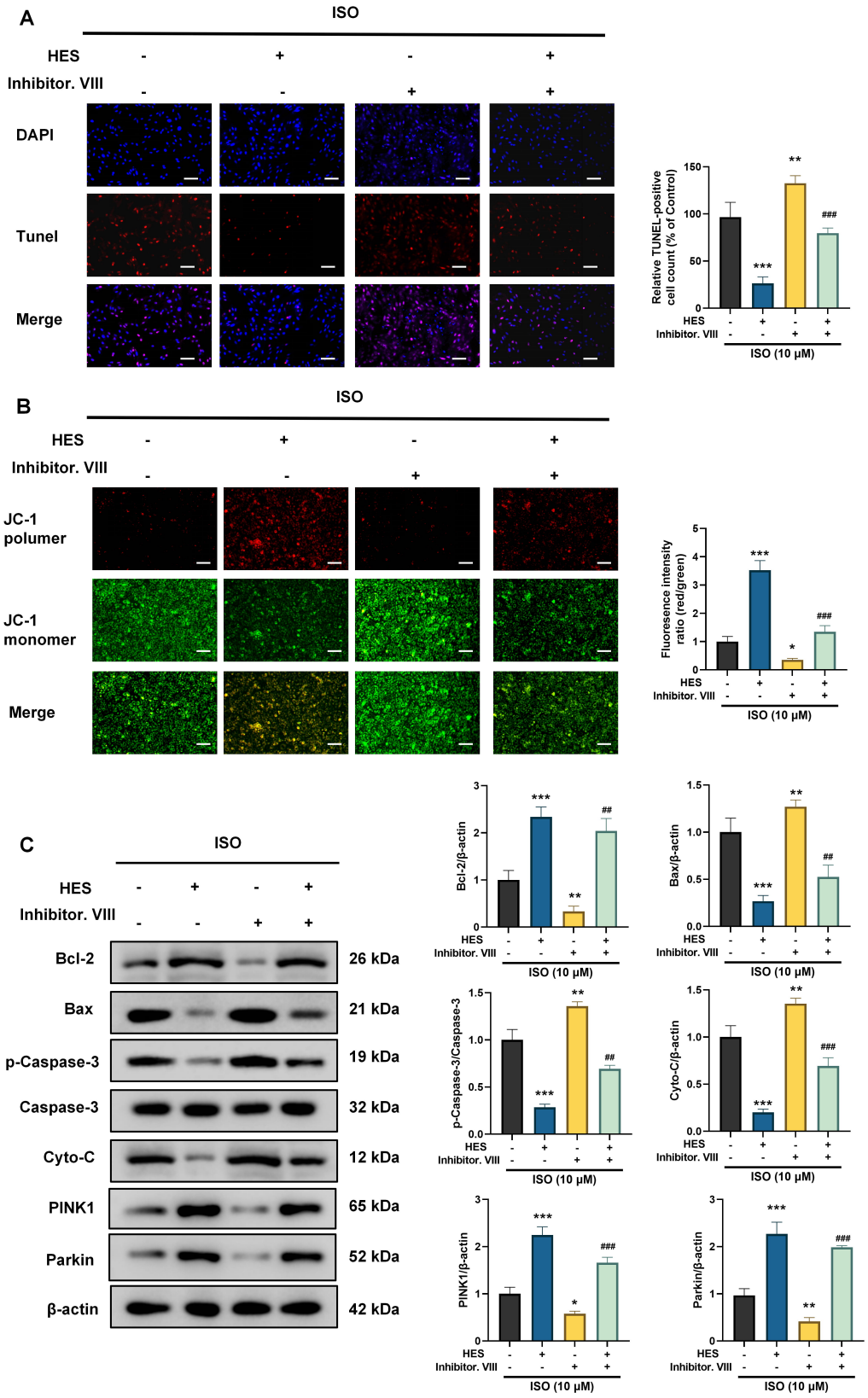

Fig. 5. Akt signaling pathway mediates the protective effects of HES against ISO-induced apoptosis in H9c2 cells. H9c2 cells subjected to different treatments: ISO, ISO + HES (20 μM), ISO + Akt inhibitor (0.1 μM), and ISO + HES (20 μM) + Akt inhibitor (0.1 μM). (A) TUNEL staining to assess cell apoptosis (200× magnification, scale bar: 50 μm). (B) JC-1 staining to evaluate MMP (200× magnification, scale bar: 50 μm). (C) WB analysis of mitochondrial apoptosis-related protein expression. Data are expressed as mean ± SD, n = 3. *$p < 0.05$, **$p < 0.01$, ***$p < 0.001$ vs. ISO group; $^{\#\#}p < 0.01$, $^{\#\#\#}p < 0.001$ vs. ISO + HES group.

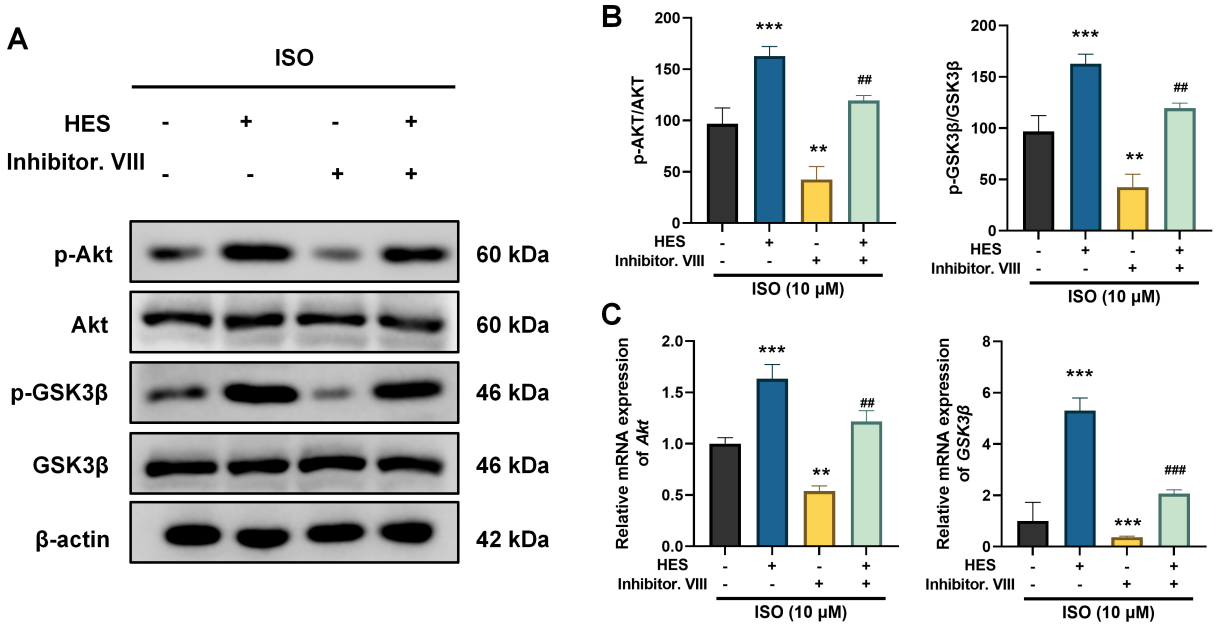

Fig. 6. Effects of Akt inhibitor VIII on HES-induced activation of the Akt/GSK3β signaling pathway. H9c2 cells subjected to different treatments: ISO, ISO + HES (20 μM), ISO + Akt inhibitor (0.1 μM), and ISO + HES (20 μM) + Akt inhibitor (0.1 μM). (A) WB assay revealing the protein expression levels pertinent to the Akt/GSK3β pathway. (B) Quantitative analysis of WB results. (C) qRT-PCR measurement of Akt and GSK3β mRNA expression in cells. Data are expressed as mean ± SD, n = 3. $^{**}p < 0.01$, $^{***}p < 0.001$ vs. ISO group; $^{\#\#}p < 0.01$, $^{\#\#\#}p < 0.001$ vs. ISO + HES group.

Discussion

Cardiovascular diseases, as prevalent global health issues, pose significant threats to human health. Myocardial cell damage is a common endpoint in various cardiovascular diseases, and therefore, highlighting the importance of identifying effective agents to ameliorate myocardial cell injury and improve clinical outcomes. ISO, a catecholamine β-adrenergic receptor agonist, when used excessively or for prolonged periods, can induce myocardial cell injury and is commonly used to establish damage models [22,23]. HES represents a flavonoid glycoside that exists within citrus fruits. Although a study has shown its protective effects against ISO-induced cardiac hypertrophy [24], research at the myocardial cellular level remains limited. In the present study, an ISO-induced *in vitro* injury model using H9c2 cardiomyocytes was established to examine the effects of HES on these cells.

Our findings indicate that HES markedly enhances the survival of H9c2 cells after exposure to ISO, improves cell vitality, and promotes cell proliferation. HES also significantly reverses ISO-induced oxidative imbalance. Previous research has shown that stimulation of the Akt signaling pathway promotes the upregulation of antioxidant defense enzymes, including HO-1 and SOD, consequently reducing oxidative stress and protecting cardiomyocytes from damage [25,26]. These findings suggest that the protective effects of HES may be partially attributed to modulation of Akt-mediated antioxidant responses.

ISO induces excessive ROS production, leading to cell apoptosis [27]. Our findings demonstrate that treatment with HES markedly decreased the percentage of ISO-induced apoptotic H9c2 myocardial cells in a dose-dependent manner ($p < 0.001$), indicating a protective effect of HES on these cells. Cyto-C is a major marker of mitochondrial-mediated apoptosis [28,29], and the increase and release of pro-apoptotic protein Cyto-C can activate caspase-3, leading to myocardial cell apoptosis [30,31]. Cyto-C release and mitochondrial activity are primarily regulated by proteins from the Bcl-2 family [32,33]. In our study, TUNEL and JC-1 staining experiments revealed that HES effectively reduced the percentage of apoptotic cells and restored mitochondrial membrane potential. WB analysis further revealed that administration of HES markedly increased the expression of the anti-apoptotic protein Bcl-2 ($p < 0.001$), while concurrently reducing the expression levels of pro-apoptotic markers, including Bax, Cytochrome C, and Caspase-3 ($p < 0.001$), indicating that HES may protect myocardial cells by inhibiting the mitochondrial apoptosis pathway. Moreover, ISO exposure markedly reduced the expression of mitochondrial quality control proteins PINK1 and Parkin, indicating impaired mitochondrial homeostasis under oxidative stress. HES treatment restored their expression, suggesting that HES alleviates mitochondrial damage and preserves mitochondrial function in ISO-treated cells.

GSK3β-regulated mitochondrial signaling and apoptosis play a critical role in myocardial ischemia [34–36]. The biological activity of GSK3β is regulated by two spe-

cific amino acid residues (Ser9 and Tyr216), and activation of Akt leads to phosphorylation of GSK3β at Ser9, resulting in its inactivation and reduction of apoptosis, thereby exerting a myocardial protective effect [37,38]. In the present investigation, HES exposure significantly elevated the phosphorylation levels of Akt and GSK3β ($p < 0.001$) in H9c2 cardiomyocytes subjected to ISO-induced injury, implying that HES may exert its protective effects by mitigating ISO-induced cellular damage through regulation of the Akt/GSK3β signaling pathway. Akt-mediated phosphorylation of GSK3β may contribute to the maintenance of mitochondrial integrity by modulating mitochondrial membrane potential, oxidative balance, and the expression of mitochondrial quality control proteins such as PINK1 and Parkin. Moreover, impaired Akt/GSK3β signaling under ISO exposure may exacerbate mitochondrial dysfunction and apoptosis, while HES restores this pathway to preserve mitochondrial homeostasis.

To further validate the role of the Akt/GSK3β signaling pathway in the protective effects of HES, we used the Akt inhibitor VIII in co-treatment experiments. The results showed that Akt inhibitor VIII partially suppressed the protective effects of HES, as compared to the ISO + HES group. The improvement in cell vitality and reduction in apoptotic cells were diminished, and HES's protective effects on oxidative stress indicators were significantly weakened. In mitochondrial function and apoptosis-related assays, Akt inhibitor VIII reduced HES's ability to restore mitochondrial membrane potential and regulate apoptosis-related protein expression. These observations further confirm that the cardioprotective effects of HES against ISO-induced myocardial injury are closely associated with its ability to regulate and activate the Akt/GSK3β signaling pathway.

Nevertheless, this study has several limitations. All experiments were conducted *in vitro*, and no *in vivo* validation was performed. Although the concentrations of HES used in this study (5–20 µM) were selected based on previous literature and demonstrated efficacy in cellular models, their physiological relevance remains uncertain. Therefore, whether the effective concentrations observed *in vitro* can be achieved *in vivo* requires further investigation. Future studies involving animal models and pharmacokinetic analyses are needed to determine the bioavailability and therapeutic potential of HES under physiological conditions.

Conclusion

In conclusion, HES mitigates ISO-induced myocardial cell injury by stimulating the Akt/GSK3β signaling pathway, alleviating oxidative stress, maintaining mitochondrial function, and inhibiting apoptosis. These findings provide valuable experimental evidence supporting the prospective use of HES for the prevention and treatment of cardiovascular diseases and offer insights into its underlying molecular mechanisms of action.

Availability of Data and Materials

The datasets generated and/or analyzed during the current study are available from the corresponding author upon reasonable request.

Author Contributions

XD: Conceptualization, Methodology, Investigation, Data curation, Writing — original draft. RC: Formal analysis, Validation, Writing — review & editing. RZ: Investigation, Data curation, Writing — review & editing. WC: Software, Formal analysis, Visualization, Writing — review & editing. BL: Visualization, Writing — review & editing. JC: Conceptualization, Supervision, Project administration, Writing — review & editing. All authors gave final approval of the version to be published. All authors have participated sufficiently in the work to take public responsibility for appropriate portions of the content and agreed to be accountable for all aspects of the work in ensuring that questions related to its accuracy or integrity.

Ethics Approval and Consent to Participate

Not applicable.

Acknowledgment

Not applicable.

Funding

This research was funded by the Science and Technology Program of Wenzhou (No. Y20240270).

Conflict of Interest

The authors declare no conflict of interest.

References

[1] The Writing Committee of the Report on Cardiovascular Health and Diseases in China. Report on Cardiovascular Health and Diseases in China 2021: An Updated Summary. Biomedical and Environmental Sciences: BES. 2022; 35: 573–603. https://doi.org/10.3967/bes2022.079.

[2] Chen J, Zhong J, Wang LL, Chen YY. Mitochondrial Transfer in Cardiovascular Disease: From Mechanisms to Therapeutic Implications. Frontiers in Cardiovascular Medicine. 2021; 8: 771298. https://doi.org/10.3389/fcvm.2021.771298.

[3] Wang Y, Ren T, Li C, Wu Q, Liu J, Guan X, *et al*. Mechanisms involved in the regulation of mitochondrial quality control by PGAM5 in heart failure. Cell Stress & Chaperones. 2024; 29: 510–518. https://doi.org/10.1016/j.cstres.2024.05.004.

[4] Li D, Zhang L, Gong Q, Deng H, Luo C, Zhou T, *et al*. The role of myocardial energy metabolism perturbations in diabetic cardiomyopathy: from the perspective of novel protein post-translational modifications. Clinical Epigenetics. 2025; 17: 15. https://doi.org/10.1186/s13148-025-01814-2.

[5] Ding Q, Qi Y, Tsang SY. Mitochondrial Biogenesis, Mitochondrial Dynamics, and Mitophagy in the Maturation of Cardiomyocytes. Cells. 2021; 10: 2463. https://doi.org/10.3390/cells10092463.

[6] Zhang Z, Chen F, Wan J, Liu X. Potential traditional Chinese medicines with anti-inflammation in the prevention of heart failure following myocardial infarction. Chinese Medicine. 2023; 18: 28. https://doi.org/10.1186/s13020-023-00732-w.

[7] Dai J, Qiu L, Lu Y, Li M. Recent advances of traditional Chinese medicine against cardiovascular disease: overview and potential mechanisms. Frontiers in Endocrinology. 2024; 15: 1366285. https://doi.org/10.3389/fendo.2024.1366285.

[8] Xie YZ, Ma J, Yao GZ, Zou X. Relationship between programmed cell death and myocardial ischemia-reperfusion injury and new perspectives of traditional Chinese medicine intervention. Zhongguo Zhong Yao Za Zhi = Zhongguo Zhongyao Zazhi = China Journal of Chinese Materia Medica. 2021; 46: 1345–1356. https://doi.org/10.19540/j.cnki.cjcmm.20201222.601. (In Chinese)

[9] Haș IM, Tit DM, Bungau SG, Pavel FM, Teleky BE, Vodnar DC, *et al*. Cardiometabolic Risk: Characteristics of the Intestinal Microbiome and the Role of Polyphenols. International Journal of Molecular Sciences. 2023; 24: 13757. https://doi.org/10.3390/ijms241813757.

[10] Pereira V, Figueira O, Castilho PC. Hesperidin: a flavanone with multifaceted applications in the food, animal feed, and environmental fields. Phytochemistry Reviews. 2025; 24: 3291–3305. https://doi.org/10.1007/s11101-024-10008-2.

[11] Sugasawa N, Katagi A, Kurobe H, Nakayama T, Nishio C, Takumi H, *et al*. Inhibition of Atherosclerotic Plaque Development by Oral Administration of α-Glucosyl Hesperidin and Water-Dispersible Hesperetin in Apolipoprotein E Knockout Mice. Journal of the American College of Nutrition. 2019; 38: 15–22. https://doi.org/10.1080/07315724.2018.1468831.

[12] Kim HK, Kim M, Marquez JC, Jeong SH, Ko TH, Noh YH, *et al*. Novel GSK-3β Inhibitor Neopetroside A Protects Against Murine Myocardial Ischemia/Reperfusion Injury. JACC. Basic to Translational Science. 2022; 7: 1102–1116. https://doi.org/10.1016/j.jacbts.2022.05.004.

[13] Bréhat J, Panel M, Ghaleb B, Morin D. Opening of mitochondrial permeability transition pore in cardiomyocytes: Is ferutinin a suitable tool for its assessment? Fundamental & Clinical Pharmacology. 2023; 37: 739–752. https://doi.org/10.1111/fcp.12879.

[14] Yan L, Cheng G, Yang G. GSKIP protects cardiomyocytes from hypoxia/reoxygenation-induced injury by enhancing Nrf2 activation via GSK-3β inhibition. Biochemical and Biophysical Research Communications. 2020; 532: 68–75. https://doi.org/10.1016/j.bbrc.2020.06.029.

[15] Zhou G, Wu H, Yang J, Ye M, Liu D, Li Y, *et al*. Liraglutide Attenuates Myocardial Ischemia/Reperfusion Injury Through the Inhibition of Necroptosis by Activating GLP-1R/PI3K/Akt Pathway. Cardiovascular Toxicology. 2023; 23: 161–175. https://doi.org/10.1007/s12012-023-09789-3.

[16] Mao S, Luo X, Li Y, He C, Huang F, Su C. Role of PI3K/AKT/mTOR Pathway Associated Oxidative Stress and Cardiac Dysfunction in Takotsubo Syndrome. Current Neurovascular Research. 2020; 17: 35–43. https://doi.org/10.2174/1567202617666191223144715.

[17] Sharma AK, Thanikachalam PV, Bhatia S. The signaling interplay of GSK-3β in myocardial disorders. Drug Discovery Today. 2020; 25: 633–641. https://doi.org/10.1016/j.drudis.2020.01.017.

[18] Chen ZQ, Zhou Y, Chen F, Huang JW, Zheng J, Li HL, *et al*. Breviscapine Pretreatment Inhibits Myocardial Inflammation and Apoptosis in Rats After Coronary Microembolization by Activating the PI3K/Akt/GSK-3β Signaling Pathway. Drug Design, Development and Therapy. 2021; 15: 843–855. https://doi.org/10.2147/DDDT.S293382.

[19] Chen ZH, Liu YX, Chen ZW, Lin MD, Zhang JL, Wang Z, *et al*. Effect and mechanism of gomisin D on the isoproterenol induced myocardial injury in H9C2 cells and mice. Journal of Asian Natural Products Research. 2024; 26: 604–615. https://doi.org/10.1080/10286020.2024.2336152.

[20] Tian M, Han YB, Zhao CC, Liu L, Zhang FL. Hesperidin alleviates insulin resistance by improving HG-induced oxidative stress and mitochondrial dysfunction by restoring miR-149. Diabetology & Metabolic Syndrome. 2021; 13: 50. https://doi.org/10.1186/s13098-021-00664-1.

[21] Li L, Aslam M, Siegler BH, Niemann B, Rohrbach S. Comparative Analysis of CTRP-Mediated Effects on Cardiomyocyte Glucose Metabolism: Cross Talk between AMPK and Akt Signaling Pathway. Cells. 2021; 10: 905. https://doi.org/10.3390/cells10040905.

[22] Fiserova I, Trinh MD, Elkalaf M, Vacek L, Heide M, Martinkova S, *et al*. Isoprenaline modified the lipidomic profile and reduced β-oxidation in HL-1 cardiomyocytes: *In vitro* model of takotsubo syndrome. Frontiers in Cardiovascular Medicine. 2022; 9: 917989. https://doi.org/10.3389/fcvm.2022.917989.

[23] Suriano C, Zerlotin R, Pignataro P, Dicarlo M, Oranger A, Zanfino L, *et al*. Irisin Treatment Prevents Isoproterenol-Induced Cardiac Fibrosis in Mice. Discovery Medicine . 2024; 36: 2202–2213.

[24] Bhargava P, Verma VK, Malik S, Khan SI, Bhatia J, Arya DS. Hesperidin regresses cardiac hypertrophy by virtue of PPAR-γ agonistic, anti-inflammatory, antiapoptotic, and antioxidant properties. Journal of Biochemical and Molecular Toxicology. 2019; 33: e22283. https://doi.org/10.1002/jbt.22283.

[25] Ren BC, Zhang YF, Liu SS, Cheng XJ, Yang X, Cui XG, *et al*. Curcumin alleviates oxidative stress and inhibits apoptosis in diabetic cardiomyopathy via Sirt1-Foxo1 and PI3K-Akt signalling pathways. Journal of Cellular and Molecular Medicine. 2020; 24: 12355–12367. https://doi.org/10.1111/jcmm.15725.

[26] Wang C, Wang P, Fu J, Yang Z, Du H, Zhang M, *et al*. Pinus massoniana pollen polysaccharides alleviate LPS-induced myocardial injury through p110β-mediated inhibition of the PI3K/AKT/NFκB pathway. International Journal of Biological Macromolecules. 2024; 283: 137713. https://doi.org/10.1016/j.ijbiomac.2024.137713.

[27] Liao M, Xie Q, Zhao Y, Yang C, Lin C, Wang G, *et al*. Main active components of Si-Miao-Yong-An decoction (SMYAD) attenuate autophagy and apoptosis via the PDE5A-AKT and TLR4-NOX4 pathways in isoproterenol (ISO)-induced heart failure models. Pharmacological Research. 2022; 176: 106077. https://doi.org/10.1016/j.phrs.2022.106077.

[28] Zhou Z, Arroum T, Luo X, Kang R, Lee YJ, Tang D, *et al*. Diverse functions of cytochrome c in cell death and disease. Cell death and differentiation. 2024; 31: 387–404. https://doi.org/10.1038/s41418-024-01284-8.

[29] Morse PT, Arroum T, Wan J, Pham L, Vaishnav A, Bell J, *et al*. Phosphorylations and Acetylations of Cytochrome *c* Control Mitochondrial Respiration, Mitochondrial Membrane Potential, Energy, ROS, and Apoptosis. Cells. 2024; 13: 493. https://doi.org/10.3390/cells13060493.

[30] Fu ZP, Wu LL, Xue JY, Zhang LE, Li C, You HJ, *et al*. Connexin 43 hyper-phosphorylation at serine 282 triggers apoptosis in rat cardiomyocytes via activation of mitochondrial apoptotic pathway. Acta Pharmacologica Sinica. 2022; 43: 1970–1978. https://doi.org/10.1038/s41401-021-00824-z.

[31] Wang X, Geng L, Wu M, Xu W, Cheng J, Li Z, *et al*. Molecular mechanisms of cardiotoxicity induced by acetamide and its chiral isomers. The Science of the Total Environment. 2023; 900:

166349. https://doi.org/10.1016/j.scitotenv.2023.166349.

[32] Popgeorgiev N, Sa JD, Jabbour L, Banjara S, Nguyen TTM, Akhavan-E-Sabet A, *et al*. Ancient and conserved functional interplay between Bcl-2 family proteins in the mitochondrial pathway of apoptosis. Science Advances. 2020; 6: eabc4149. https://doi.org/10.1126/sciadv.abc4149.

[33] Yu P, Shi L, Song M, Meng Y. Antitumor activity of paederosidic acid in human non-small cell lung cancer cells via inducing mitochondria-mediated apoptosis. Chemico-biological Interactions. 2017; 269: 33–40. https://doi.org/10.1016/j.cbi.2017.02.003.

[34] Ajzashokouhi AH, Rezaee R, Omidkhoda N, Karimi G. Natural compounds regulate the PI3K/Akt/GSK3β pathway in myocardial ischemia-reperfusion injury. Cell Cycle (Georgetown, Tex.). 2023; 22: 741–757. https://doi.org/10.1080/15384101.2022.2161959.

[35] Li Y, Lu R, Niu Z, Wang D, Wang X. Suxiao Jiuxin Pill alleviates myocardial ischemia-reperfusion injury through the ALKBH5/GSK3β/mTOR pathway. Chinese Medicine. 2023; 18: 31. https://doi.org/10.1186/s13020-023-00736-6.

[36] Boovarahan SR, Kurian GA. Preconditioning the rat heart with 5-azacytidine attenuates myocardial ischemia/reperfusion injury via PI3K/GSK3β and mitochondrial K_{ATP} signaling axis. Journal of Biochemical and Molecular Toxicology. 2021; 35: e22911. https://doi.org/10.1002/jbt.22911.

[37] Zhang X, Lu Z, Abdul KSM, Changping MA, Tan KS, Jovanovi A, *et al*. Isosteviol sodium protects heart embryonic H9c2 cells against oxidative stress by activating Akt/GSK-3β signaling pathway. Die Pharmazie. 2020; 75: 36–40. https://doi.org/10.1691/ph.2020.9851.

[38] Wang LY, Tang DD, Li RL, Li MY, He LS, Pu XF, *et al*. Extraction process optimization of Ligusticum chuanxiong hort. and its cardiomyocyte-protective effects via regulation of Dvl-1/Akt/GSK-3β/Nrf2. Arabian Journal of Chemistry. 2024; 17: 105843.